Four-Legged Piano Stool Molybdenum(II) Compounds without Carbonyl Ligands. 4. Cyclopentadienylmolybdenum(II) Complexes with 16-Electron and 18-Electron Configurations

Fatima Abugideiri, James C. Fettinger, D. Webster Keogh, and Rinaldo Poli*

Department of Chemistry and Biochemistry, University of Maryland,
College Park, Maryland 20742

Received May 3, 1996[⊗]

Monocyclopentadienyl complexes of Mo(II) with 16- and 18-electron configurations of the form (Ring)MoClL$_x$ (x = 2, Ring = Cp, L = PMe_2Ph; x = 2, Ring = Cp*, L = PMe_3, PMe_2Ph, L_2 = dppe; x = 3, Ring = Cp, L = PMe_2Ph) are described. All of the 16-electron complexes are paramagnetic with an $S = 1$ ground state, as shown by magnetic measurements in the solid state and in solution, and by the contact-shifted ^{1}H NMR spectra. The structure of Cp*MoCl(dppe) was determined by X-ray diffraction methods. The 18-electron complex $CpMoCl(PMe_2Ph)_3$ has been synthesized by reduction of $\{CpMoCl_2\}_n$ with Na in the presence of 3 equiv of phosphine. It has been fully characterized by ^{1}H and ^{31}P NMR, chemical analysis, and X-ray structural determination. Thermolysis of a THF or C_6D_6 solution of this 18-electron species generates the 16-electron paramagnetic Mo(II) complex $CpMoCl(PMe_2Ph)_2$. The Cp^*MoClL_2 (L = PMe_3 and PMe_2Ph) systems react with 2-electron-donor ligands, i.e. CO and H_2, to afford stable 18-electron complexes. The carbonyl derivative $Cp^*MoCl(CO)(PMe_2Ph)_2$ has also been characterized by X-ray crystallography.

Introduction

We are interested in the effect of the spin state on the energetic stabilization of electronically unsaturated organometallic complexes. For instance, a 16-electron complex might have the 2 electrons of highest energy unpaired and located 1 each in the two highest energy orbitals of the valence shell, giving rise to a spin triplet, or they may be paired in the same orbital, leaving a relatively accessible LUMO:

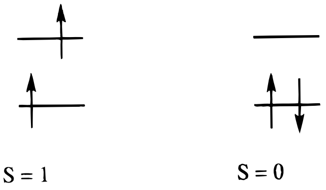

A similar situation may be pictured for 15-electron complexes, where the choice is between an $S = {}^1/_2$ and an $S = {}^3/_2$ configuration.

The electronic configuration has profound effects on the reactivity of the molecule; for instance, an $S = 0$ 16-electron complex has the ability to undergo rapid ligand additions or oxidative-addition reactions, whereas the same reactions on the spin triplet counterpart should be slower because they involve a forbidden (in principle)[1] crossover to the singlet state of the 18-electron product. The energetics of stable molecules and reaction intermediates (and therefore the reaction thermodynamics, kinetics, and mechanism) can also be affected by spin changes.[2] We therefore wish to study phenomenologically the factors that determine the choice of spin state.

In simple terms, the choice between the above two electronic configurations is determined by the relative magnitude of the separation between the two orbitals and the pairing energy. Given a certain energetic separation between the two orbitals in question, the low effective positive charge on the metal center in typical low-oxidation-state organometallic compounds results in diffuse metal orbitals and therefore low pairing energies, favoring the low-spin configuration. Low-oxidation-state 16-electron complexes are typically reactive intermediates which easily engage in ligand-addition or oxidative-addition reactions. In most instances, the assumption is implicitly made in the literature that such intermediates have a low-spin configuration, or the question of their spin state is simply not addressed. There are, however, important cases of high-spin intermediates, for instance $Fe(CO)_4$ and CpCo(CO).[3−5]

For higher oxidation state complexes, the higher effective positive charge on the metal center is expected to result in a greater pairing energy and a higher relative stability of the high-spin configuration with respect to the alternative low-spin one. A good example is provided by the isostructural and isoelectronic series of four-legged piano stool, d^2 (16-electron) compounds of Zr(II), $(\eta^6\text{-}C_6H_5Me)ZrCl_2(PMe_3)_2$[6] (diamagnetic), Nb(III), $Cp^*NbCl_2(PMe_3)_2$[7] (paramagnetic), and Mo(IV),

---

[⊗] Abstract published in *Advance ACS Abstracts,* September 1, 1996.

[1] Detrich, J. L.; Reinaud, O. M.; Rheingold, A. L.; Theopold, K. H. *J. Am. Chem. Soc.* **1995**, *117*, 11745−11748.

[2] Poli, R. *Comments Inorg. Chem.* **1992**, *12*, 285−314.

[3] Poliakoff, M.; Weitz, E. *Acc. Chem. Res.* **1987**, *20*, 408−414.

[4] Bengali, A. A.; Bergman, R. G.; Moore, C. B. *J. Am. Chem. Soc.* **1995**, *117*, 3879−3880.

[5] Siegbahn, P. E. M. *J. Am. Chem. Soc.* **1996**, *118*, 1487−1496.

[6] Diamond, G. M.; Green, M. L. H.; Walker, N. M.; Howard, J. A. K.; Mason, S. A. *J. Chem. Soc., Dalton Trans.* **1992**, 2641−2647.

[7] Siemeling, U.; Gibson, V. C. *J. Organomet. Chem* **1992**, *424*, 159−161.

$[CpMoCl_2(PMe_3)_2]^+$ (paramagnetic).[8] Since pairing energies are lower for more diffuse orbitals, a higher spin state is more likely observed for an unsaturated complex of a 3d metal versus the 4d and 5g congeners. The isoelectronic intermediates CpM(CO) (M = Co, Rh) illustrate the dramatic difference in chemical reactivity for species with different spin: while the $S = 0$ CpRh(CO) rapidly binds 2-electron-donor ligands (even the inert gases Kr and Xe!) and oxidatively add C−H bonds of saturated hydrocarbons,[9,10] the corresponding $S = 1$ CpCo(CO) fragment does not engage in either process.[4] We have shown that the phosphine ligand exchange on the 17-electron ($S = {}^1/_2$) $CpMoX_2L_2$ complexes (X = halogen; L = tertiary phosphine) occurs via the 15-electron intermediate $CpMoX_2L$ (rather than through the associative mechanism which is typical of low-oxidation-state radicals) and advanced the hypothesis that a spin state change to a more favorable $S = {}^3/_2$ configuration is at least in part responsible for this change of mechanism.[11] We shall address elsewhere how pairing energies affect the relative stabilities of 15-electron spin quartet $CpMCl_2(PH_3)$ versus 17-electron spin doublet $CpMCl_2(PH_3)_2$ for M = Cr, Mo.[12]

We have now embarked on a synthetic project designed to probe the stability and spin state of electronically unsaturated organometallic complexes in different oxidation states. We have found that for the Mo(IV) $(\eta\text{-}C_5R_5)MoCl_3L_n$ system, when the less sterically encumbered Cp and L = PMe_3, PMe_2Ph ligands are employed, an equilibrium is established between the 18-electron $CpMoCl_3L_2$ and the 16-electron spin triplet $CpMoCl_3L$ complexes, whereas only the 16-electron mono(phosphine) adduct could be obtained for the sterically more encumbered Cp* systems and also for the Cp system with the bulkier phosphine $PMePh_2$.[13] Also, the stable 16-electron $[CpMoCl_2(PMe_3)_2]^+$ complex reacts promptly and quantitatively with Cl^- to afford $CpMoCl_3(PMe_3)_2$ (in equilibrium with $CpMoCl_3(PMe_3)$), whereas $[CpMoI_2(PMe_3)_2]^+$ and I^- do not show any tendency to form the corresponding 18-electron adduct.[14,15] All these 16-electron four-legged piano stool Mo(IV) complexes have a spin triplet ground state.

For the Mo(III) $(\eta\text{-}C_5R_5)MoCl_2L_n$ system, we have not yet been able to produce a stable 15-electron monophosphine adduct, whereas a number of 17-electron bisadducts have been obtained, isolated, and characterized.[16] We have shown that this is not due to insufficient stabilization of the alleged $(\eta\text{-}C_5R_5)MoCl_2L$ complex by the expected $S = {}^3/_2$ electronic configuration with respect to the bis(phosphine) adduct but rather to a ligand disproportionation reaction to ultimately afford the thermodynamically more favorable combination of $(\eta\text{-}C_5R_5)MoCl_2L_2$ and $[(\eta\text{-}C_5R_5)MoCl_2]_2$.[17]

Here we report the results of our investigations on the class of Mo(II) complexes of general formula $(\eta\text{-}C_5R_5)MoClL_n$, for which either an 18-electron ($n = 3$) or a 16-electron ($n = 2$) configuration is expected. The lowering of the metal oxidation state from Mo(IV) to Mo(III) to Mo(II) is of interest because (i) the preference for a high-spin electronically unsaturated configuration should decrease and (ii) lower coordination numbers are sufficient to achieve electronic saturation; therefore, electronically unsaturated complexes can be assumed to be less dependent on steric effects (e.g. compare the three-legged piano stool $CpMoClL_2$ with the four-legged piano stool $CpMoCl_3L$, both having a 16-electron count). Our studies demonstrate that 16-electron Mo(II) complexes (i) unlike the 15-electron Mo(III) $CpMoX_2L$ complexes[17] are stable in solution and (ii) like the 16-electron Mo(IV) $CpMoCl_3L$ systems preferably adopt a high-spin configuration. Part of this work has been previously communicated.[18]

Experimental Section

General Data. All operations were carried out under an atmosphere of argon. Solvents were dehydrated by conventional methods and distilled directly from the dehydrating agent prior to use (THF and Et_2O from Na/benzophenone, heptane and toluene from Na, and CH_2Cl_2 from P_2O_5). NMR spectra were recorded on Bruker WP200 and AF200 spectrometers; the peak positions are reported with positive shifts downfield of TMS as calculated from the residual solvent peaks (^1H) or downfield of external 85% H_3PO_4 (^{31}P). For each ^{31}P NMR spectrum, a sealed capillary containing H_3PO_4 was immersed in the same NMR solvent used for the measurement and this was used as the external reference. EPR spectra were recorded on a Bruker ER200 spectrometer equipped with an X-band microwave generator. Cyclic voltammograms were recorded with an EG&G 362 potentiostat connected to a Macintosh computer through MacLab hardware/software; the electrochemical cell was a locally modified Schlenk tube with a Pt counter electrode sealed through uranium glass/Pyrex glass seals. The cell was fitted with a Ag/AgCl reference electrode and a Pt working electrode. All potentials are reported vs the Cp_2Fe/Cp_2Fe^+ couple, which was introduced into the cell at the end of each measurement. The solid-state magnetic susceptibility measurements were performed with a Johnson Matthey magnetic susceptibility balance. The elemental analyses were by M-H-W Laboratories, Phoenix, AZ or Galbraith Laboratories, Inc., Knoxville, TN. Cp^*MoCl_4,[17,19] $Cp^*MoCl_2(PMe_3)_2$,[20] $Cp^*MoCl(PMe_3)_2(N_2)$,[20] $\{CpMoCl_2\}_n$,[21] and $Cp^*MoCl(PMe_3)_3$[22] were prepared by literature methods. PMe_3 (Aldrich), PMe_2Ph (Aldrich), dppe (Strem), H_2 (Air Products), and CO (Air Products) were used without further purification.

Preparation of $CpMoCl(PMe_2Ph)_3$ (1) and Formation of $CpMoCl(PMe_2Ph)_2$ (2). $\{CpMoCl_2\}_n$ (306 mg, 1.32 mmol) and THF (25 mL) were introduced into a Schlenk tube equipped with a magnetic stirring bar, and PMe_2Ph (563 μL, 547 mg, 3.96 mmol; PMe_2Ph/Mo ratio 3.0) was added to the

---

[8] Krueger, S. T.; Poli, R.; Rheingold, A. L.; Staley, D. L. *Inorg. Chem.* **1989**, *28*, 4599−4607.

[9] Schultz, R. H.; Bengali, A. A.; Tauber, M. J.; Weiller, B. H.; Wasserman, E. P.; Kyle, K. R.; Moore, C. B.; Bergman, R. G. *J. Am. Chem. Soc.* **1994**, *116*, 7369−7377.

[10] Bengali, A. A.; Schultz, R. H.; Moore, C. B.; Bergman, R. G. *J. Am. Chem. Soc.* **1994**, *116*, 9585−9589.

[11] Cole, A. A.; Fettinger, J. C.; Keogh, D. W.; Poli, R. *Inorg. Chim. Acta* **1995**, *240*, 355−366.

[12] Cacelli, I.; Poli, R.; Rizzo, A. To be submitted for publication.

[13] Abugideiri, F.; Gordon, J. C.; Poli, R.; Owens-Waltermire, B. E.; Rheingold, A. L. *Organometallics* **1993**, *12*, 1575−1582.

[14] Poli, R.; Owens, B. E.; Linck, R. G. *J. Am. Chem. Soc.* **1992**, *114*, 1302−1307.

[15] Poli, R.; Rheingold, A. L.; Owens-Waltermire, B. E. *Inorg. Chim. Acta* **1993**, *203*, 223−227.

[16] Poli, R. *J. Coord. Chem. B* **1993**, *29*, 121−173.

[17] Abugideiri, F.; Keogh, D. W.; Kraatz, H.-B.; Poli, R.; Pearson, W. *J. Organomet. Chem.* **1995**, *488*, 29−38.

[18] Abugideiri, F.; Keogh, D. W.; Poli, R. *J. Chem. Soc., Chem. Commun.* **1994**, 2317−2318.

[19] Murray, R. C.; Blum, L.; Liu, A. H.; Schrock, R. R. *Organometallics* **1985**, *4*, 953−954.

[20] Baker, R. T.; Calabrese, J. C.; Harlow, R. L.; Williams, I. D. *Organometallics* **1993**, *12*, 830−841.

[21] Linck, R. G.; Owens, B. E.; Poli, R.; Rheingold, A. L. *Gazz. Chim. Ital.* **1991**, *121*, 163−168.

[22] Abugideiri, F.; Kelland, M. A.; Poli, R.; Rheingold, A. L. *Organometallics* **1992**, *11*, 1303−1311.

resulting suspension, which was then stirred until the CpMoCl$_2$ precipitate reacted with PMe$_2$Ph to form CpMoCl$_2$(PMe$_2$Ph)$_2$ (ca. 1 h), according to published procedures.[23] The solution was transferred using a filter cannula into a Schlenk tube containing amalgamated Na (30 mg, 1.32 mmol in 11 g of Hg). The mixture was stirred for 4 days, the color changing from purple-brown to orange-brown, and then filtered through Celite. The solvent was removed under reduced pressure, and the residue was extracted with toluene (200 mL), filtered, and placed in a −20 °C freezer for 10 days. The resulting red crystals were filtered and dried in vacuo. Yield: 218 mg, 27%. Anal. Calcd for C$_{29}$H$_{38}$ClMoP$_3$: C, 57.01; H, 6.27. Found: C, 56.80; H 6.25. ^{1}H NMR (C$_6$D$_6$, δ): 7.6−6.7 (m, 15H, PPh), 4.59 (d, 5H, $J_{\mathrm{H-P}} = 2$ Hz, Cp), 1.82 (vt, 6H, $J_{\mathrm{H-P}} = 7$ Hz, P−CH$_3$), 1.43 (vt, 6H, $J_{\mathrm{H-P}} = 6$ Hz, P−CH$_3$), 0.73 (d, 6H, $J_{\mathrm{H-P}} = 3$ Hz, PMe$_2$Ph). ^{31}P NMR (C$_6$D$_6$, δ): 34.7 (t, 1P, $J_{\mathrm{P-P}} = 53$ Hz), 21.9 (d, 2P, $J_{\mathrm{P-P}} = 53$ Hz). Crystals for the X-ray analysis were obtained by extraction of the crude material into Et$_2$O and cooling overnight at −20 °C.

In a repeat experiment which was run under identical conditions starting from 578 mg (2.49 mmol) of {CpMoCl$_2$}$_2$, 115 mg (4.98 mmol) of Na amalgamated with 20 g of Hg, and 1.10 mL (7.48 mmol) of PMe$_2$Ph in 90 mL of THF, the solution obtained after filtration from Celite was evaporated to dryness and the residue was extracted with *n*-heptane (70 mL). After filtration, the solution was once more evaporated to dryness and the residue was crystallized from 40 mL of Et$_2$O at −80 °C, giving 540 mg of a brown solid. ^{1}H NMR inspection of this solid revealed that it mainly consists of a paramagnetic species, with CpMoH(PMe$_2$Ph)$_3$ impurity (ca. 5% by NMR integration). ^{1}H NMR (C$_6$D$_6$, δ): (a) resonances assigned to CpMoCl(PMe$_2$Ph)$_2$, 21.5 (br s, $w_{1/2} = 79$ Hz, 4H, *o*-Ph), 16.6 (br s, $w_{1/2} = 80$ Hz, 12H, PMe), 10.9 (br s, $w_{1/2} = 25$ Hz, 2H, *p*-Ph), 0.85 (br s, $w_{1/2} = 42$ Hz, 4H, *m*-Ph); (b) resonances attributed to CpMoH(PMe$_2$Ph)$_3$, ca. 7 (m, Ph), 4.47 (s, 5H, Cp), 1.37 (d, 18H, Me, $J_{\mathrm{P-H}} = 2.1$ Hz), −7.7 (q, 1H, Mo-H, $J_{\mathrm{H-P}} = 51$ Hz).

Thermal Treatment of Compound 1. A sample of **1** (20 mg, 0.033 mmol) was dissolved in C$_6$D$_6$ (ca. 1 mL). The resulting solution was warmed to 45 °C in a sealed NMR tube for 6 h. ^{1}H and ^{31}P{^{1}H} NMR analyses showed the presence of a mixture of starting material, free PMe$_2$Ph (Me resonance at δ 1.12 in the ^{1}H spectrum and resonance at δ −45.5 in the ^{31}P{^{1}H} spectrum), and CpMoCl(PMe$_2$Ph)$_2$ (paramagnetically shifted resonances identical with those listed above). Continued heating resulted in a complete loss of the paramagnetically shifted peaks and to the formation of a complicated mixture of diamagnetic products which were not further investigated (^{1}H NMR resonances in the Cp region at δ 5.24, 4.66, 4.46, 4.36, and 4.04).

Synthesis of Cp*MoCl(PMe$_3$)$_2$ (3). Cp*MoCl$_4$ (0.511 g, 1.37 mmol) was added to a THF solution (40 mL) of amalgamated Na (0.098 g, 4.26 mmol, in 9 g of Hg) and PMe$_3$ (0.284 mL, 2.74 mmol). After it was stirred overnight, the resulting yellow-brown solution was evaporated to dryness, the residue extracted with heptane (25 mL), and the extract filtered through Celite until the washings were colorless. The compound could not be crystallized out of solutions of saturated hydrocarbons, and these solutions were therefore used directly for the derivatization reactions with CO, H$_2$, and PMe$_3$ (vide infra). The concentration of Cp*MoCl(PMe$_3$)$_2$ was determined by reacting an aliquot of the heptane solution with H$_2$ to afford Cp*MoCl(H)$_2$(PMe$_3$)$_2$ quantitatively and gas-volumetrically measuring the amount of gas absorbed. On the basis of this procedure the yield was 41%. ^{1}H NMR (C$_6$D$_6$, δ): 44.8 (br s, $w_{1/2} = 105$ Hz, 15H, C$_5$Me$_5$), 17.8 (br s, $w_{1/2} = 55$ Hz, 18 H, PMe$_3$). μ_{eff} (Evans' method) = 2.94 μ_{B}. An alternative to amalgamated Na is using Na sand (3 mol/mol of Cp*MoCl$_4$) and naphthalene (0.3−0.5 mol/mol of Cp*MoCl$_4$).

Synthesis of Cp*MoCl(PMe$_2$Ph)$_2$ (4). In a procedure identical with that described above for the preparation of **3**, Cp*MoCl$_4$ (0.105 g, 0.282 mmol) was added to a THF solution (15 mL) of amalgamated Na (0.021 g, 0.913 mmol, in 2 g of Hg) and PMe$_2$Ph (0.080 mL, 0.564 mmol). After it was stirred overnight, the resulting orange-brown solution was evaporated to dryness and the residue was extracted with heptane (20 mL) and filtered through Celite until the washings were colorless. The compound could not be crystallized out of solutions of saturated hydrocarbons, and these solutions were therefore used directly for the derivatization reactions with CO, H$_2$, and PMe$_3$ (vide infra). ^{1}H NMR (C$_6$D$_6$, δ): 71 (br s, $w_{1/2} = 230$ Hz, 15 H, C$_5$Me$_5$), 16.3 and 15.3 (1:1 br s, $w_{1/2} = 115$ Hz, 12 H, P*Me$_2$*Ph). 8.9 (s, $w_{1/2} = 22$ Hz, 2 H, *p*-Ph), 7.8 (s, $w_{1/2} = 26$ Hz, 4 H, *m*-Ph), 6.1 (s, $w_{1/2} = 150$ Hz, 4 H, *o*-Ph).

Synthesis of Cp*MoCl(dppe) (5). Cp*MoCl$_4$ (0.234 g, 0.627 mmol) was added to Na (0.049 g, 2.13 mmol), naphthalene (0.015 g, 0.117 mmol), dppe (0.249 g, 0.625 mmol), and THF (15 mL). After it was stirred for 2 days, the orange solution was evaporated to dryness. The residue was extracted with hot heptane (4 × 10 mL) and the extract filtered through Celite. The solution was placed at −80 °C overnight, which precipitated an orange microcrystalline solid. The solid was filtered, dried, and isolated. Yield: 0.260 g, 62%. Anal. Calcd for C$_{36}$H$_{39}$ClMoP$_2$: C, 65.02; H, 5.91. Found: C, 65.19; H, 6.01. ^{1}H NMR (C$_6$D$_6$, δ): 75.5 (br s, $w_{1/2} = 50$ Hz, 4 H, *o*-Ph), 62.6 (br s, $w_{1/2} = 150$ Hz, 15 H, C$_5$Me$_5$). 15.2 and 11.9 (s, $w_{1/2} = 22$ Hz, 8 H, *m*-Ph), 14.6 (br s, $w_{1/2} = 90$ Hz, 4 H, *o*-Ph), 6.4 and 4.3 (s, 4 H, *p*-Ph), −1.2 (br s, $w_{1/2} = 118$ Hz, 4 H, Ph$_2$P*CH$_2$CH$_2$*PPh$_2$). $\mu_{\mathrm{eff}} = 2.65$ μ_{B}. A single crystal for X-ray analysis of Cp*MoCl(dppe) was obtained by dissolving the crude product in hot heptane, filtering, and cooling the solution to room temperature slowly in an oil bath.

Thermal Decomposition of 3. A sample of **3** prepared as described above was dissolved in C$_6$D$_6$ and the solution sealed in an NMR tube and heated to 85 °C for $^1/_2$ h, then an additional 2 h at 100 °C, and finally to 135 °C with ^{1}H and ^{31}P NMR monitoring after each heating. After the complete heating period the ^{1}H NMR indicated the complete decomposition of **3**. The final ^{1}H and ^{31}P NMR spectra showed the typical resonances[24] of Cp*MoH(PMe$_3$)$_3$.

Reaction of Cp*MoCl$_2$L$_2$ with Na. (a) L = PMe$_3$. Equimolar quantities of Cp*MoCl$_2$(PMe$_3$)$_2$ and amalgamated Na (ca. 0.5%) were allowed to react in THF (ca. 0.02 M) with ^{1}H NMR monitoring by periodically withdrawing an aliquot of the solution, evaporating it to dryness, and redissolving it in the NMR solvent (C$_6$D$_6$). After 1−2 days, the ^{1}H NMR spectrum indicated the complete disappearance of the resonance at δ −2.3 of Cp*MoCl$_2$(PMe$_3$)$_2$ and conversion to the 16-electron Cp*MoCl(PMe$_3$)$_2$ complex (**3**).

(b) L = PMe$_2$Ph. Equimolar quantities of Cp*MoCl$_2$(PMe$_2$Ph)$_2$ and amalgamated Na (ca. 0.5%) were allowed to react in THF (ca. 0.02 M) with ^{1}H NMR monitoring by periodically withdrawing an aliquot of the solution, evaporating it to dryness, and redissolving it in the NMR solvent (C$_6$D$_6$). After 1−2 days the ^{1}H NMR spectrum indicated the complete conversion to the 16-electron Cp*MoCl(PMe$_2$Ph)$_2$ complex (**4**). Solutions of this compound were used directly for the derivatization reactions with CO, H$_2$, and PMe$_3$ (vide infra).

Thermal Treatment of Cp*MoCl(PMe$_3$)$_3$. A sample of Cp*MoCl(PMe$_3$)$_3$ (67 mg, 0.135 mmol) was dissolved in C$_6$D$_6$ (ca. 2 mL). The resulting solution was warmed to 60 °C in a sealed NMR tube with periodical monitoring by ^{1}H and ^{31}P{^{1}H} NMR. After 5.5 h, ^{1}H and ^{31}P{^{1}H} NMR analyses showed the presence of a mixture of starting material, free PMe$_3$, and compound **3**. After a total of 17 h of heating a mixture similar to that before was observed, but the resonances of **3** had diminished in intensity and new resonances of the thermal decomposition product of **3** (vide supra) were present as well as an increase in the resonance at δ −2.3 for Cp*MoCl$_2$(PMe$_3$)$_2$.

Reaction between Cp*MoClL$_2$ and CO. (a) L = PMe$_3$. Formation of *trans*-Cp*MoCl(PMe$_3$)$_2$(CO) (6). A solution

---

[23] Poli, R.; Owens, B. E.; Krueger, S. T.; Rheingold, A. L. *Polyhedron* **1992**, *11*, 2301−2312.

[24] Abugideiri, F.; Kelland, M. A.; Poli, R. *Organometallics* **1992**, *11*, 1311−1318.

Table 1. Crystal Data for Compounds 1, 5, and 7

compd	$CpMoCl(PMe_2Ph)_3$, **1**	$Cp^*MoCl(dppe)$, **5**	$Cp^*MoCl(CO)(PMe_2Ph)_2$, **7**
formula	$C_{29}H_{38}ClMoP_3$	$C_{36}H_{39}ClMoP_2$	$C_{27}H_{37}ClMoOP_2$
fw	610.89	665.00	570.93
space group	$P2_1/n$	$P2_1/n$	$P2_1/c$
a, Å	11.7902(8)	11.1404(12)	9.572(2)
b, Å	15.2863(11)	17.628(2)	13.461(2)
c, Å	16.2122(11)	16.936(2)	21.452(3)
β, deg	105.288(6)	107.922(9)	97.84(2)
V, Å^3	2818.5(3)	3164.7(5)	2738(2)
Z	4	4	4
d_{calc}, g/cm^3	1.440	1.396	1.38
μ(Mo Kα), cm^{-1}	7.44	6.24	7.02
radiation (monochromated in incident beam)	Mo Kα (λ = 0.710 73 Å)	Mo Kα (λ = 0.710 73 Å)	Mo Kα (λ = 0.710 73 Å)
temp, K	153	153	296
transmissn factors: max, min	0.9686, 0.8644	0.9627, 0.8029	1.000, 0.958
R^a	0.0611	0.0365	0.0459
Rw^b	0.1067	0.0812	0.0551

[a] $R = \sum||F_o| - |F_c||/\sum|F_o|$. [b] $R_w = [\sum w(|F_o| - |F_c|)^2/\sum w|F_o|^2]^{1/2}$; $w = 1/\sigma^2(|F_o|)$.

of $Cp^*MoCl(PMe_3)_2$ obtained in situ as described above from 0.660 mmol of $Cp^*MoCl_2(PMe_3)_2$ was evaporated to dryness, and the residue was extracted in pentane (20 mL). The resulting solution was filtered and then exposed to CO at 1 atm. The formation of a brown precipitate occurred immediately, which was then filtered off. Spectroscopic investigations of the mother liquor indicated the presence of compound **6**. MS (CI, negative ions; *m*/*e*): 448 ([M]$^-$, 100%), 372 ([M]$^-$ − PMe_3, 93%). IR (pentane, cm^{-1}): 1786. ^1H NMR (C_6D_6, δ): 1.66 (s, 15H, Cp*), 1.30 (vt, J_{PH} = 4 Hz, 18H, PMe_3). $^{31}P\{^1H\}$ NMR (C_6D_6, δ): 18.5.

(b) L = PMe_2Ph. Formation of *trans*-$Cp^*MoCl(PMe_2Ph)_2(CO)$ (7). A solution of $Cp^*MoCl(PMe_2Ph)_2$ obtained in situ as described above from 0.520 mmol of $Cp^*MoCl_2(PMe_2Ph)_2$ was evaporated to dryness, and the residue was extracted in ether (20 mL). The resulting solution was filtered and then exposed to CO at 1 atm. The solution immediately changed color from yellow-brown to orange-brown. Cooling to −20 °C over 1 week afforded 65 mg of compound **7** (27% yield), which was isolated by decanting off the mother liquor and drying under vacuum. Anal. Calcd for $C_{27}H_{37}ClMoOP_2$: C, 56.80; H, 6.53; Cl, 6.21. Found: C, 56.4; H, 6.9; Cl, 6.9. IR (pentane, cm^{-1}): 1793. ^1H NMR (C_6D_6, δ): 7.79 (m , 4 H, PMe_2Ph), 7.08 (m, 6 H, PMe_2Ph), 1.52 (s, 15H, Cp*), 1.44 (overlap of 2 vt, 12 H, PMe_2Ph). $^{31}P\{^1H\}$ NMR (C_6D_6, δ): 22.0. A single crystal for X-ray analysis of $Cp^*MoCl(PMe_2Ph)_2(CO)$ was obtained by cooling a pentane solution to −80 °C.

Reaction between Cp^*MoClL_2 and H_2. (a) L = PMe_3. Preparation of $Cp^*MoClH_2(PMe_3)_2$ (8). $Cp^*MoCl(PMe_3)_2(N_2)$ (0.340 g, 0.761 mmol) was dissolved in heptane (20 mL) and the solution exposed to an atmosphere of H_2. After the blue solution was heated to 45 °C for 1 h, the solution became red. The absence of ν_{N-N} in the IR confirmed the complete consumption of the starting material. The heptane solution was concentrated to half the original volume and placed at −80 °C overnight, precipitating a red-brown solid. The solid was filtered and dried under vacuum. Yield: 0.140 g, 44%. Anal. Calcd for $C_{16}H_{35}ClMoP_2$: C, 45.67; H, 8.39. Found: C, 45.56; H, 8.39. ^1H NMR (C_6D_6, δ): 1.76 (s, 15 H, C_5Me_5), 1.32 (d, 18 H, J_{PH} = 9 Hz, PMe_3), −2.83 (t, 2H, J_{PH} = 50 Hz, MoH_2). $^{31}P\{selective\text{-}^1H\}$ NMR (δ): 11.0 (t, J_{PH} = 38 Hz).

This compound was also generated by an alternative method, i.e. addition of H_2 to $Cp^*MoCl(PMe_3)_2$, although it was not isolated from this procedure. A solution of $Cp^*MoCl(PMe_3)_2$ obtained in situ as described above from 0.44 mmol of $Cp^*MoCl_2(PMe_3)_2$ was evaporated to dryness, and the residue was extracted in heptane (20 mL) and filtered. The resulting solution was then stirred at room temperature under an atmosphere of H_2, resulting in no apparent color change. After 3 h, an aliquot of the solution was inspected by NMR after evaporation to dryness and redissolution in C_6D_6, confirming the formation of compound **8** as the major product. The ^1H NMR also showed the presence of $Cp^*MoCl_2(PMe_3)_2$ (broad resonance at δ −2.3), which was present prior to the reaction with H_2.

(b) L = PMe_2Ph. Formation of $Cp^*MoClH_2(PMe_2Ph)_2$ (9). A solution of $Cp^*MoCl(PMe_2Ph)_2$ obtained in situ as described above from 0.52 mmol of $Cp^*MoCl_2(PMe_2Ph)_2$ was evaporated to dryness, and the residue was extracted in heptane (20 mL) and the extract filtered. The resulting solution was then stirred at room temperature under an atmosphere of H_2, resulting in no apparent color change. After 3 h, an aliquot of the solution was inspected by NMR after evaporation to dryness and redissolution in C_6D_6, confirming the formation of compound **9** as the major product. ^1H NMR (C_6D_6, δ): 1.71 (s, 15 H, C_5Me_5), 1.46 (d, 12 H, J_{PH} = 10 Hz, PMe_2Ph), −2.23 (t, 2H, J_{PH} = 50 Hz, MoH_2). $^{31}P\{selective\text{-}^1H\}$ NMR (δ): 21.8 (t, J_{PH} = 34 Hz). Other resonances in the ^1H and ^{31}P NMR spectra were due to free PMe_2Ph and to other unidentified diamagnetic and paramagnetic complexes.

X-ray Crystallography. (a) $CpMoCl(PMe_2Ph)_3$ (1). A reddish purple crystal with dimensions 0.225 × 0.200 × 0.038 mm was placed and optically centered on the Enraf-Nonius CAD-4 diffractometer. The parameters and crystal orientation matrix were determined from 25 reflections in the range $17.5 < \theta < 19.8°$ and confirmed with axial photographs. Data were collected with $\omega/2\theta$ scans over the range $2.25 < \theta < 24.0°$. No decay correction was necessary. An absorption correction was applied on the basis of crystal faces with transmission factors ranging from 0.8644 to 0.9686. The uniquely determined centrosymmetric monoclinic space group $P2_1/n$ was indicated by the systematic absences from the data and confirmed by the successful completion of the structure. After data reduction and correction for Lorentz and polarization factors, direct methods successfully located all the non-hydrogen atoms. All hydrogen atoms were found from an initial difference-Fourier map; however, hydrogen atoms attached to carbon atoms were placed instead in calculated positions, with $d(C-H_3)$ = 0.980 Å and $U_H = 1.5U$(parent) and with aromatic d(C−H) = 0.950 Å and $U_H = 1.2U$(parent). All of the non-hydrogen atoms were refined anisotropically by full-matrix least-squares cycles. Crystal data are reported in Table 1, and selected bond distances and angles are collected in Table 2.

(b) $Cp^*MoCl(dppe)$ (5). A reddish purple crystal with dimensions 0.375 × 0.375 × 0.050 mm was placed and optically centered on the Enraf-Nonius CAD-4 diffractometer. The cell parameters and crystal orientation matrix were determined from 25 reflections in the range $16.0 < \theta < 19.3°$; these constants were confirmed with axial photographs. Data were collected (Mo Kα) with $\omega/2\theta$ scans over the range $2.25 < \theta < 24.0°$. No decay correction was necessary. Data were cor-

Table 2. Selected Intramolecular Distances (Å) and Angles (deg) for $CpMoCl(PMe_2Ph)_3$ (1)

Mo(1)−CNT[a]	1.974(9)	Mo(1)−P(1)	2.486(2)
Mo(1)−P(2)	2.453(2)	Mo(1)−Cl(1)	2.585(2)
Mo(1)−P(3)	2.459(2)		
CNT[a]−Mo(1)−Cl(1)	109.9(2)	P(1)−Mo(1)−P(3)	84.01(8)
CNT[a]−Mo(1)−P(1)	120.0(3)	P(2)−Mo(1)−P(3)	85.20(8)
CNT[a]−Mo(1)−P(2)	114.7(3)	P(1)−Mo(1)−Cl(1)	72.75(8)
CNT[a]−Mo(1)−P(3)	114.3(2)	P(2)−Mo(1)−Cl(1)	77.79(8)
P(1)−Mo(1)−P(2)	123.72(8)	P(3)−Mo(1)−Cl(1)	135.74(8)

[a] CNT is the center of gravity of atoms C(1)−C(5).

Table 3. Selected Bond Distances (Å) and Angles (deg) for Cp*MoCl(dppe) (5)

Mo(1)−CNT[a]	1.998(5)	Mo(1)−P(1)	2.428(1)
Mo(1)−Cl(1)	2.416(1)	Mo(1)−P(2)	2.413(1)
CNT[a]−Mo(1)−Cl(1)	120.1(1)	Cl(1)−Mo(1)−P(1)	83.59(4)
CNT[a]−Mo(1)−P(1)	136.8(1)	Cl(1)−Mo(1)−P(2)	92.94(5)
CNT[a]−Mo(1)−P(2)	129.6(1)	P(1)−Mo(1)−P(2)	78.71(4)

[a] CNT is the center of gravity of atoms C(1)−C(5).

Table 4. Selected Bond Distances (Å) and Angles (deg) for $Cp^*MoCl(CO)(PMe_2Ph)_2$

Mo−Cl	2.577(5)	Mo−Cl(A)	2.616(10)
Mo−P(1)	2.479(2)	Mo−P(2)	2.469(2)
Mo−C(O)	1.874(11)	Mo−C(OA)	1.887(15)
Mo−C(17)	2.342(8)	Mo−C(18)	2.304(8)
Mo−C(19)	2.298(8)	Mo−C(20)	2.352(9)
Mo−C(21)	2.377(9)	Mo−CNT[a]	2.017(9)
P(1)−C(1)	1.827(8)	P(1)−C(2)	1.815(8)
P(1)−C(3)	1.830(8)	P(2)−C(9)	1.833(8)
P(2)−C(10)	1.841(9)	P(2)−C(11)	1.827(7)
C(O)−O	1.114(15)	C(OA)−OA	1.104(17)
Cl−Mo−P(1)	79.7(1)	Cl−Mo−P(2)	76.5(1)
Cl−Mo−C(O)	130.2(4)	Cl−Mo−CNT[a]	111.9(4)
Cl(A)−Mo−P(1)	76.0(2)	Cl(A)−Mo−P(2)	75.6(2)
Cl(A)−Mo−C(OA)	128.9(7)	Cl(A)−Mo−CNT[a]	119.1(4)
P(1)−Mo−P(2)	116.6(1)	P(1)−Mo−C(O)	76.2(4)
P(1)−Mo−C(OA)	76.8(7)	P(1)−Mo−CNT[a]	122.1(4)
P(2)−Mo−C(O)	76.6(4)	P(2)−Mo−C(OA)	79.2(7)
P(2)−Mo−CNT[a]	121.2(4)	C(O)−Mo−CNT[a]	117.8(5)
C(OA)−Mo−CNT[a]	111.9(8)	Mo−C(O)−O	173.4(13)
Mo−C(OA)−OA	175(3)		

[a] CNT = centroid of atoms C(17)−C(21).

rected for Lorentz and polarization factors, and an absorption correction was applied on the basis of crystal faces with transmission factors ranging from 0.8029 to 0.9627. The uniquely determined centrosymmetric monoclinic space group $P2_1/n$ was indicated by the systematic absences from the data and confirmed by the successful completion of the structure. Direct methods successfully located all of the heavy atoms (Mo, P, Cl) and many of the carbon atoms. All remaining non-hydrogen atoms were found from an initial difference-Fourier map and/or had their positions calculated. Hydrogen atoms were treated as described in the previous section for compound **1**. Crystal data are assembled in Table 1, and selected bond distances and angles are collected in Table 3.

(c) $Cp^*MoCl(CO)(PMe_2Ph)_2$ (7). A single crystal was glued to the inside of a thin-walled glass capillary, which was then flame-sealed under dinitrogen and mounted on the diffractometer. The cell determination, data collection, and reduction were carried out as described above for compound **5**. The position of the Mo atom was obtained from the analysis of the Patterson map, and the positions of all the other non-hydrogen atoms were revealed by a subsequent DIRDIF run. The structure was then refined by least-squares cycles to convergence with all non-hydrogen atoms anisotropic. The final difference-Fourier map revealed disorder with a minor orientation of the two relative trans Cl and CO ligands in the opposite configuration (e.g. the Cl of the minor species occupies the same coordination position as the CO of the major species and vice versa). Both major and minor orientations were introduced at variable occupancies, which were refined independently (Cl, x; ClA, $1 - x$; C and O, y; CA and OA, $1 - y$). In order to avoid instability, the following distances were restrained with DFIX cards in SHELX76: Mo−Cl = Mo−ClA = 2.58(5) Å; Mo−C(O) = Mo−C(OA) = 1.94(2) Å; C(O)−O = C(OA)−OA = 1.15(2) Å. Refinement converged to $R = 0.0544$ with all atoms except ClA and the carbonyl C and O atoms for both major and minor orientations anisotropic, giving $x = 0.66$ and $y = 0.74$, confirming the correctness of the model. Finally, x and y were constrained to have the same value as dictated by stoichiometry and the hydrogen atoms were included in calculated positions as described above for the structure of **1**. Crystal data are reported in Table 1, and selected bond distances and angles are collected in Table 4.

Results

Synthesis and Spectroscopic Characterization of (Ring)MoClL$_2$. Solutions of the paramagnetic, 16-electron (Ring)MoClL$_2$ complexes (Ring = Cp, L = PMe$_2$Ph (**2**); Ring = Cp*, L = PMe$_3$ (**3**), PMe$_2$Ph (**4**), L$_2$ = dppe (**5**)) were obtained by four different methods: (i) by reduction of Cp^*MoCl_4 in the presence of L (eq 1), (ii) by reduction of $Cp^*MoCl_2L_2$ (eq 2), (iii) by reduction of $CpMoCl_2$ in the presence of L (eq 3) (this reaction probably proceeds by initial coordination of the phosphine ligand to generate the 17-electron $CpMoCl_2L_2$ complexes, followed by reduction as for the corresponding Cp* systems in eq 2), and (iv) by thermal ligand dissociation from the 18-electron complexes $CpMoCl(PMe_2Ph)_3$ and $Cp^*MoCl(PMe_3)_3$ (eq 4).

$$Cp^*MoCl_4 + 3Na + 2L \xrightarrow{THF,\ Ar} Cp^*MoClL_2 + 3NaCl \quad (1)$$
$$L = PMe_3,\ PMe_2Ph;\ L_2 = dppe$$

$$Cp^*MoCl_2L_2 + Na \xrightarrow{THF,\ Ar} Cp^*MoClL_2 + NaCl \quad (2)$$
$$L = PMe_3,\ PMe_2Ph$$

$$CpMoCl_2 + Na + 2PMe_2Ph \xrightarrow{THF,\ Ar} CpMoCl(PMe_2Ph)_2 + NaCl \quad (3)$$

$$(Ring)MoClL_3 \xrightarrow{\Delta,\ C_6D_6} (Ring)MoClL_2 + L \quad (4)$$
$$Ring = Cp,\ L = PMe_2Ph;\ Ring = Cp^*,\ L = PMe_3$$

Compounds **2**−**4** could not be isolated in the crystalline state and were charcacterized by spectroscopy and by chemical derivatization (vide infra). However, compound **5** was isolated as a crystalline solid and characterized by ^{1}H NMR, elemental (C,H) analysis, magnetic susceptibility, and X-ray crystallography.

The ^{1}H NMR spectra for all of the 16-electron complexes show broad paramagnetically shifted resonances. Figure 1a shows the ^{1}H NMR spectrum of compound **3**. The broad resonance ($w_{1/2}$ = 105 Hz) at 45 ppm is assigned to the Cp* ligand, whereas the peak at 18 ppm ($w_{1/2}$ = 55 Hz) is assigned to the PMe$_3$ ligand. The qualitative features of this spectrum are identical in other NMR solvents (i.e. acetone-d_6) or in the presence of THF. As expected, the 16-electron complexes are EPR-silent, since the two possible spin states are $S = 1$ and $S = 0$. Systems with more than one unpaired electron are generally EPR-inactive due to large zero-field splittings and fast electronic relaxations. Com-

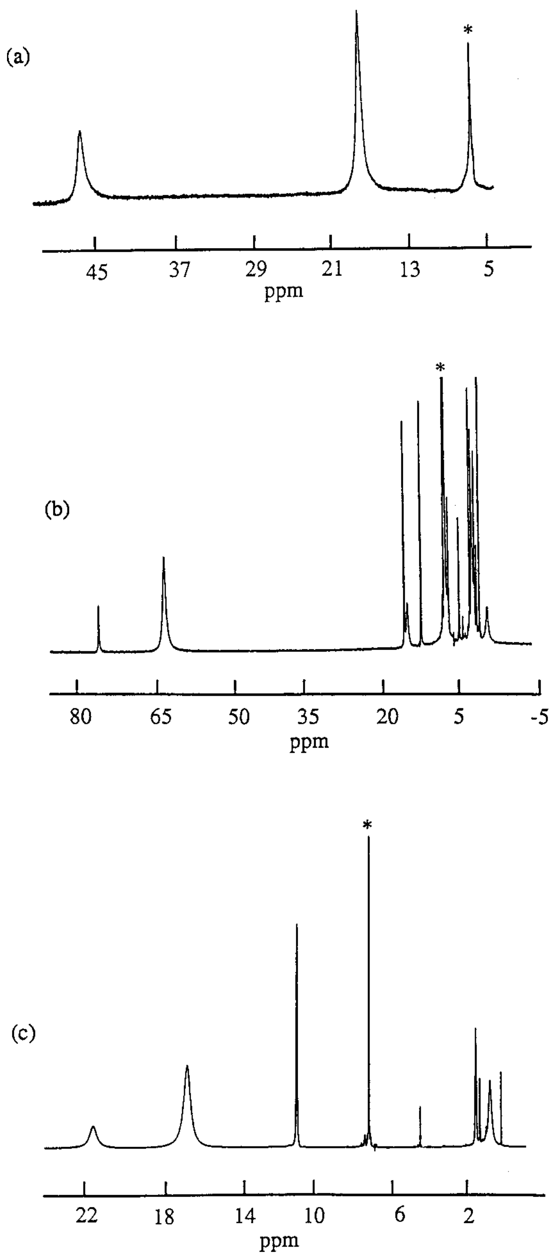

Figure 1. ^{1}H NMR of (a) Cp*MoCl(PMe_3)$_2$ (**3**), (b) Cp*MoCl(dppe) (**5**), and (c) CpMoCl(PMe_2Ph)$_2$ (**2**). All spectra were recorded in C_6D_6. The starred resonance corresponds to C_6D_5H.

pound **4** also shows a broad and strongly shifted Cp* resonance in the ^{1}H NMR spectrum (at δ 71 with $w_{1/2}$ = 230 Hz). The diastereotopic methyl protons of the PMe_2Ph ligands are obeserved at δ 16.3 and 15.3 ($w_{1/2}$ = 115 Hz). The phenyl protons also show paramagnetically shifted and broadened peaks: the ortho protons at δ 6.1 ($w_{1/2}$ = 150 Hz), the meta at δ 7.8 ($w_{1/2}$ = 26 Hz), and the para at δ 8.9 ($w_{1/2}$ = 22 Hz). The assignment is based on relative line widths (the protons closest to the paramagnetic metal center, i.e. ortho, have the broader resonance) and relative intensity (the para protons are half the intensity of the meta protons).

The analysis of the ^{1}H NMR spectrum of compound **5** (see Figure 1b) also deserves some attention, especially with respect to the phenyl protons of the dppe ligand. The broad resonance at 63 ppm ($w_{1/2}$ = 150 Hz) is assigned to the Cp* ligand and compares well with that found for **3** and **4**. The symmetry of the molecule dictates two equal sets of phenyl and methylene resonances, one set being for the two rings and methylene protons pointing toward the Cp* ligand and the other set for those directed away from it. As a result, the dppe ligand should exhibit a total of eight resonances in a 4:4, 4:4, 2:2, and 2:2 ratio for the two sets of ortho, meta, para, and methylene protons, respectively. The resonances assigned to the ortho protons are at 76 ppm ($w_{1/2}$ = 50 Hz) and 15 ppm ($w_{1/2}$ = 90 Hz). It is interesting to note the large difference in the shifts of these two resonances, much larger than for all of the other types of protons. This can be attributed to a large difference in through-space dipolar interaction with the electronic spins. The meta and para protons show much less differences in chemical shifts, i.e. 3.0 and 2.1 ppm, respectively.

The preparation of **1** follows the procedure previously reported for the preparation of the related CpMoCl(PMe_3)$_3$.[22] The yield of this product is low, being crystallized from Et_2O at low temperatures. A large amount of more soluble material remained in solution, and no additional significant amount of **1** was recovered upon further concentration and cooling. The more soluble material was recovered by crystallization from very concentrated ether solutions (see Experimental Section). It consists of the paramagnetic compound CpMoCl(PMe_2Ph)$_2$ (**2**), along with small amounts of the hydride complex CpMoH(PMe_2Ph)$_3$ as an impurity. The latter is recognized from the diagnostic hydride resonance, split into a binomial quartet by coupling to the three equivalent phosphorus nuclei, at δ −7.7 in the ^{1}H NMR spectrum. The ^{1}H NMR spectrum of **2** (see Figure 1c), like the other 16-electron complexes described above, shows paramagnetically shifted and broadened resonances. The Cp ligand was so broadened and/or contact-shifted that it could not be detected. The analysis of the relative intensities and line widths led to the reasonable assignment of the δ 16.6 ($w_{1/2}$ = 80 Hz) resonance to the PMe_2Ph methyl protons and the δ 21.5 ($w_{1/2}$ = 79 Hz), 10.9 ($w_{1/2}$ = 25 Hz), and 0.85 ($w_{1/2}$ = 42 Hz) resonances to the PMe_2Ph ortho, para, and meta protons, respectively. The thermal treatment of **1** in C_6D_6 for several hours produces an observable quantity of the same paramagnetic product **2** (eq 4). The proposed phosphine dissociation/association process must be sufficiently slow on the NMR time scale because **1** and **2** are independently observed. The analogous equilibrium between the 18-electron Cp*MoCl(PMe_3)$_3$ and the paramagnetic **3** is also quite slow.[18] The exact position of the equilibrium that is established by heating the 18-electron tris(phosphine) compound could not be determined due to the formation of Cp*MoCl$_2$(PMe_3)$_2$ as well as Cp*MoH(PMe_3)$_3$, the thermal decomposition products of **3**.

Magnetic Properties. The paramagnetism observed for the solutions of **2-5** (as indicated by the paramagnetically shifted resonances in the ^{1}H NMR) suggests a spin triplet ground state. The solid-state magnetic moment of **5** was determined to be 2.65 μ_B. This is in excellent agreement with the theoretical spin-only value of 2.83 μ_B. As stated above, the other 16-electron species could not be crystallized. However, the magnetic moment of **3** could be determined in solution as μ_{eff} = 2.93 μ_B by the Evans method. One of the concerns with systems of this type is the presence of a spin equilibrium. This occurs when the energy gap

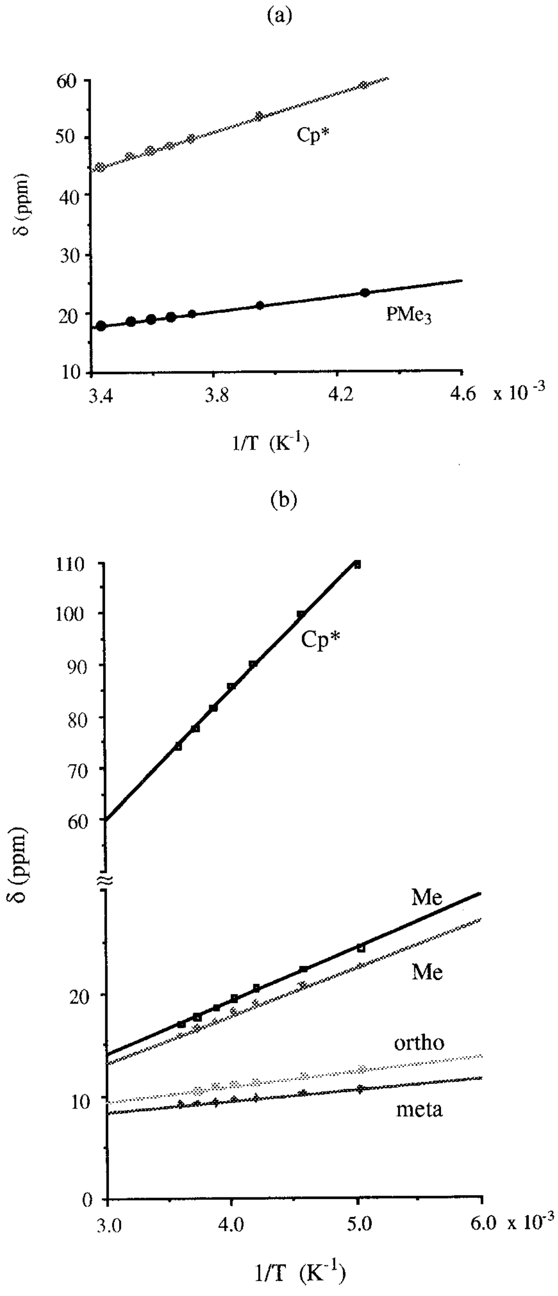

Figure 2. Plot of δ versus T^{-1} for (a) $Cp^*MoCl(PMe_3)_2$ (**3**) and (b) $Cp^*MoCl(PMe_2Ph)_2$ (**4**).

between the ground state and the excited state is small enough to allow thermal population of the latter. In order to probe for this possibility, variable-temperature NMR experiments were carried out on compounds **3** and **4**. As the temperature was lowered, the resonances for the paramagnetic protons became broader and more contact-shifted as expected. Figure 2 shows the dependence of the chemical shift versus T^{-1}. The observed linear behavior indicates that the system follows Curie–Weiss behavior and therefore excludes a significant thermal population of an excited singlet state.

Reaction of Cp^*MoClL_2 with CO and H_2. Treatment of solutions of compounds **3** and **4** with CO (eq 5) gives rise to formation of the 18-electron CO adducts $Cp^*MoCl(CO)L_2$ ($L = PMe_3$ (**6**), PMe_2Ph (**7**)), and treatment with H_2 (eq 6) gives rise to the formation of the products of H–H oxidative addition, the Mo(IV) complexes $Cp^*MoClH_2L_2$ ($L = PMe_3$ (**8**), PMe_2Ph (**9**)). These 18-electron H_2 and CO adducts are less soluble than the 16-electron precursors, allowing in some cases isolation in the crystalline state. Compound **5** also forms a CO adduct, as already described elsewhere.[25]

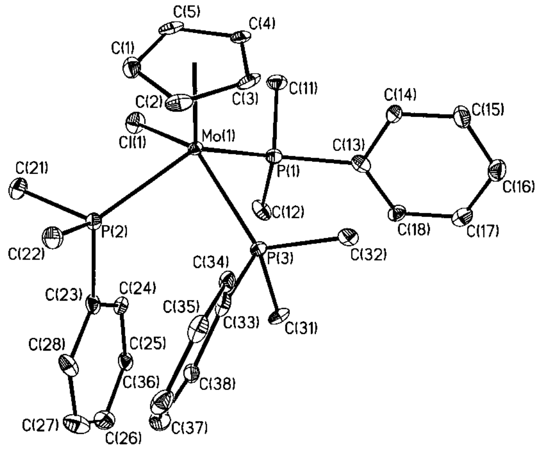

Figure 3. ORTEP diagram of $CpMoCl(PMe_2Ph)_3$ (**1**).

$$Cp^*MoClL_2 + CO \xrightarrow{THF} Cp^*MoClL_2(CO) \qquad (5)$$
$$L = PMe_3,\ PMe_2Ph$$

$$Cp^*MoClL_2 + H_2 \xrightarrow{THF} Cp^*MoCl(H)_2L_2 \qquad (6)$$
$$L = PMe_3,\ PMe_2Ph$$

The CO adducts **6** and **7** were characterized by IR and ^1H and ^{31}P NMR spectroscopy, and by an X-ray analysis of **7**. The CO stretching vibrations are observed at 1786 cm^{-1} for **6** and 1793 cm^{-1} for **7**, in agreement with the greater basicity of the PMe_3 ligand as compared to PMe_2Ph. Each compound shows a single phosphorous resonance in the ^{31}P NMR and a virtual triplet resonance in the ^1H NMR for the phosphine methyl protons, indicating equivalent phosphines in a trans geometry. This structural supposition is further confirmed by the X-ray analysis of **7** (vide infra).

The ^1H and ^{31}P NMR properties of **8** and **9** are fully consistent with the formation of a classical Mo(IV) dihydride complex with rapidly exchanging H ligands. Each compound shows a singlet for the Cp* resonance, a doublet for the methyl resonances of the phosphine ligand, and a triplet for the MoH_2 resonances, indicating coupling to two equivalent phosphines. The $^{31}P\{^1H$-selective$\}$ NMR spectra show a single triplet resonance, confirming the conclusion that, on the NMR time scale, the two phosphorus nuclei are equivalent and are coupled to two equivalent hydrides. The NMR properties of these chloro/dihydride complexes correspond quite closely to those of $(C_5H_4$-*i*-$Pr)MoClH_2(PMe_3)_2$, which was shown to have a single hydride resonance for the two rapidly exchanging inequivalent classical hydride ligands at room temperature, which decoalesced upon cooling to low temperature.[26]

X-ray Analyses. The structures of compounds **1**, **5**, and **7** have been determined by X-ray diffraction methods. Views of the three molecules are in Figures 3–5, respectively. The geometry of **5** is a typical three-legged piano stool; this is the first reported structure for a

---

(25) Fettinger, J. C.; Keogh, D. W.; Poli, R. *J. Am. Chem. Soc.* **1996**, *118*, 3617–3625.

(26) Grebenik, P. D.; Green, M. L. H.; Izquierdo, A.; Mtetwa, V. S. B.; Prout, K. *J. Chem. Soc., Dalton Trans.* **1987**, 9–19.

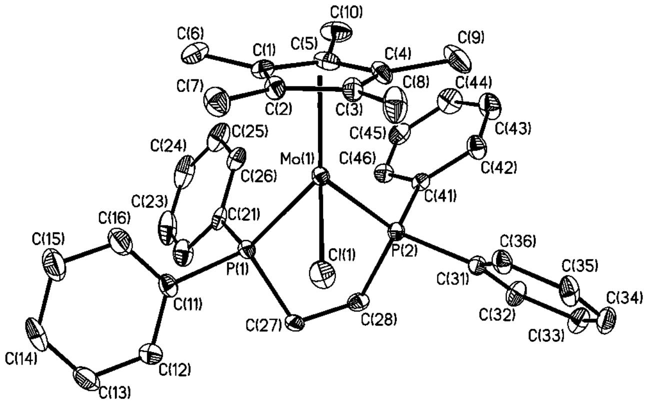

Figure 4. ORTEP diagram of Cp*MoCl(dppe) (**5**).

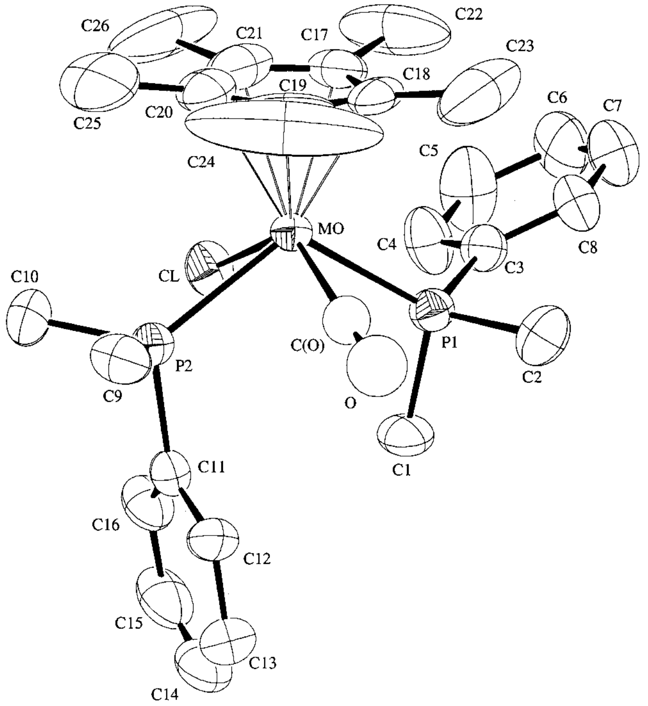

Figure 5. ORTEP diagram of Cp*MoCl(CO)($PMe_2Ph)_2$ (**7**).

paramagnetic, 16-electron, organometallic Mo(II) complex. The average L−M−L angle is 85.1(1)°, which compares with the value of 84.7(2)° for the diamagnetic $CpW(CO)_2(POCMe_2CMe_2O)$. The average CNT−Mo−L angle (CNT is the Cp ring centroid), i.e. 129(1)°, is significantly larger than for four-legged piano stool compounds, i.e. 115(1)° for **1**. One of the other expected structural characteristics is a shorter Mo-Cl length (2.416(1) Å) compared to 18-electron Mo(II) four-legged species (e.g. 2.585(2) Å for **1** and 2.526(2) Å for CpMoCl(triphos) (triphos = $Ph_2PCH_2CH_2P(Ph)CH_2CH_2PPh_2$)).[27] A much less significant difference is observed for the Mo−P lengths, those of **5** (average 2.420(1) Å) being only slightly shorter than for **1** (average 2.466(2) Å).

Molecular geometries of **1** and **7** are based on the "four-legged piano stool", which is ubiquitous for compounds of the $CpML_4$ type.[28,29] The structure of **1** is one of the first structures for a fully phosphine-substituted $CpMoXL_3$ complex (X = any one-electron donor), the only other being that of CpMoCl(triphos).[27] The most interesting angular parameters are the angles between the Mo-CNT vector and the other bonds. In the structure of **1**, the two relative trans donors Cl and P2 have smaller angles than the other donors P1 and P3. This follows the established pattern of angular trans influence,[29] which places the pair of ligands with overall stronger σ-bonding ability at smaller angles in order to maximize the interaction with the more favorable metal orbitals.[30] This angular trans influence was also observed in the structure of CpMoCl(triphos).[27] The Mo−Cl distance is significantly longer in compound **1** (2.58(1) Å) compared to CpMoCl(triphos) (2.526(2) Å), but is in each case longer than for the Mo(III) complex $[CpMoCl(PMe_3)_3]^+$ (2.427(9) Å in the PF_6^- salt[22] and 2.509(3) Å in the BF_4^- salt[31]), as expected. A longer Mo−Cl bond length is also observed in **7** (2.577(5) Å), this being comparable to the same distance in **1**. Other relevant four-legged piano stool Mo(II) complexes also show longer Mo−Cl distances (e.g. 2.541(5) Å in CpMoCl(CO)(dppe)[32] and 2.542(9) Å in $CpMoCl(CO)_3$[33]). The Mo−P distances are slightly shorter for **1** (average 2.46(1) Å) than for CpMoCl(triphos) (average 2.48(1) Å) with the length for **7** (2.470(2) Å) falling directly in between. A comparison with other literature values (2.388(8) Å in $(C_5H_4Me)MoI(CO)_2[P(OMe_3)_3]$,[34] 2.50(1) Å in $CpMoI(CO)_2(PBu_3)$,[35] 2.532(6) Å in $CpMoBr(CO)_2(PPh_3)$,[36] 2.473(3) Å in $CpMo(COCH_3)(CO)_2(PPh_3)$,[37] and 2.47(3) Å in CpMoCl(dppe)(CO)[32]) suggests that the Mo−P bonds tend to shorten when more phosphine and fewer CO ligands are present in the coordination sphere (consistent with diminished π-competition), and a further shortening effect is also due to the presence of chelate rings. A similar effect is also observable for the M−C(O) bond length, which is shorter in compound **7** (1.88(2) Å) than the average distance in other compounds with less donating ancillary ligands: 1.938(18) Å in CpMoCl(dppe)(CO),[32] 1.94(6) Å in $CpMoI(CO)_2(PBu_3)$,[35] 1.951(13) Å in $CpMo(COCH_3)(CO)_2(PPh_3)$,[37] 2.003(34) Å in $(C_5H_4Me)MoI(CO)_2[P(OMe_3)_3]$,[34] and 2.091(14) Å in $CpMoBr(CO)_2(PPh_3)$.[36]

Discussion

Half-sandwich 18-electron complexes of Mo(II) constitute a very extensive class of compounds.[38,39] Related complexes with a 16-electron configuration are rare, and most, especially when they contain one or more CO ligands, have only been observed as transients in chemical reactions. For instance, the $CpMoX(CO)_2$ (X = Cl, CH_3) fragments are obtained by photolytic CO ejection from $CpMoX(CO)_3$, but the primary photoproduct rapidly reacts with N_2, C_2H_4, CO, and other sub-

---

(27) Cole, A. A.; Mattamana, S. P.; Poli, R. *Polyhedron* **1996**, *15*, 2351−2361.

(28) Kubácek, P.; Hoffmann, R.; Havlas, Z. *Organometallics* **1982**, *1*, 180−188.

(29) Poli, R. *Organometallics* **1990**, *9*, 1892−1900.

(30) Lin, Z.; Hall, M. B. *Organometallics* **1993**, *12*, 19−23.

(31) Fettinger, J. C.; Kraatz, H.-B.; Poli, R.; Rheingold, A. L. *Acta Crystallogr., Sect. C* **1995**, *C51*, 364−367.

(32) Bush, M. A.; Hardy, A. D. U.; Manojlovic-Muir, L.; Sim, G. A. *J. Chem. Soc. A* **1971**, 1003−1009.

(33) Chaiwaise, S.; Fenn, R. H. *Acta Crystallogr., Sect. B* **1968**, *B24*, 525−5219.

(34) Hardy, A. D. U.; Sim, G. A. *J. Chem. Soc., Dalton Trans.* **1972**, 1900−1903.

(35) Fenn, R. H.; Cross, J. H. *J. Chem. Soc. A* **1971**, 3312−3315.

(36) Sim, G. A.; Sime, J. G.; Woodhouse, D. I.; Knox, G. R. *Acta Crystallogr., Sect. B* **1979**, *B35*, 2403−2406.

(37) Churchill, M. R.; Fennessey, J. P. *Inorg. Chem.* **1968**, *7*, 953−959.

(38) Wilkinson, G.; Stone, F. G. A.; Abel, E. W. *Comprehensive Organometallic Chemistry*; Pergamon: Oxford, U.K., 1982.

(39) Wilkinson, G.; Stone, F. G. A.; Abel, E. W. *Comprehensive Organometallic Chemistry II*; Pergamon: Oxford, U.K., 1995.

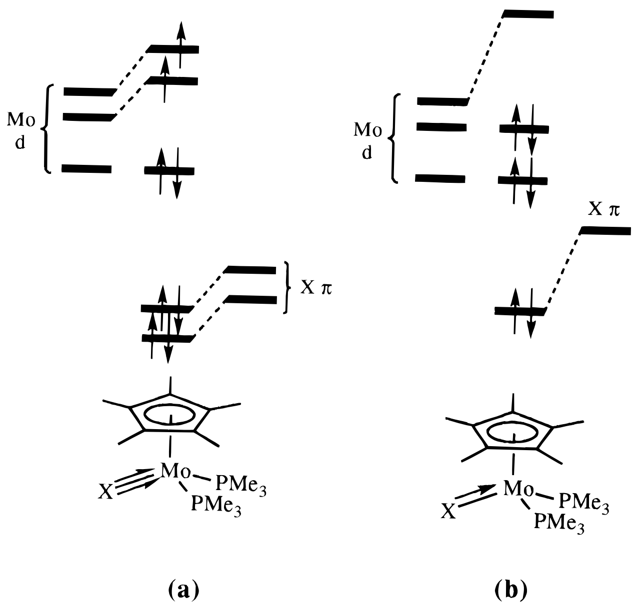

Figure 6. Qualitative MO diagram for the M−X π interaction: (a) interation with the double-sided Cl; (b) interaction with the single-sided PR_2.

strates to afford saturated adducts.[40−42] Rare examples of stable 16-electron complexes are based on the general formula (Ring)$MoXL_2$, where Ring is Cp or a substituted derivative, L is CO or phosphine, and X is an efficient π-donor group such as a phosphido or arsenido ligand.[20,43−45] Consequently, all these complexes are effectively electronically saturated and are diamagnetic. Nevertheless, some of them readily add ligands to form 18-electron adducts. The complexes **2**−**5** reported in this contribution are the first organometallics of Mo(II) to be stable as spin triplet ground states for a 16-electron configuration.

It is interesting to compare the spin triplet compound Cp*$MoCl(PMe_3)_2$ with the previouly reported spin singlet compounds Cp*$Mo(PR_2)(PMe_3)_2$ (R = Ph, cyclohexyl).[20] This spin state difference can be rationalized on the basis of differences in frontier orbital gaps and pairing energies. Considering these complexes in a similar light as low-valent organometallics with covalent bonding, the open-shell configuration can gain stability through π-bonding. Chlorine is a double-sided π-donor and is therefore capable of interacting with and raising the energy of two of the frontier metal orbitals (see Figure 6a). Consequently, the gap between the two highest orbitals is small. Conversely, the phosphide is a single-sided π-donor and is only able to raise the energy of one metal orbital (Figure 6b), resulting in a larger energy gap between the two highest metal-based orbitals. From the point of view of pairing energies, it has to be recognized that the chlorine atom has a higher electronegativity than the PR_2 function; thus, a greater effective positive charge on the metal center is expected, causing contraction of the metal-based orbitals and therefore a greater pairing energy. The spin state difference between the 6-coordinate, 14-electron derivatives *trans*-$TiX_2(dmpe)_2$ ($S = 1$ for X = Cl; $S = 0$ for X = CH_3)[46] has analogously been attributed to smaller pairing energies in the dimethyl compound because of the lower electronegativity of CH_3 relative to Cl.[47] These Cp*$MoX(PMe_3)_2$ systems are isolobal with the known trans-octahedral $MoCl_2(PMe_3)_4$,[48] which shows the expected triplet ground state for the pseudo-$t_{2g}{}^4$ configuration.

It is important to realize that, although each Mo−Cl π interaction is rendered less effective by the antibonding electron with respect to the single Mo−PR_2 π-interaction, the overall Mo−Cl π-donation is still worth 2 electrons and contributes to the energetic stabilization of the molecule. This is most clearly indicated by the significant contraction of the Mo−Cl bond on going from the 18-electron **1** and **7** to the 16-electron **5** (see Results). For this reason, we represented the Mo−Cl π-interactions as two single-pointed arrows in Figure 6a.

The 16-electron complexes (Ring)$MoClL_2$ react with 2-electron-donor ligands, i.e. CO and H_2, to afford stable saturated 18-electron complexes. It has also been shown earlier that **3** reacts with N_2 to afford an 18-electron dinitrogen adduct.[18] These reactions involve a spin state change from $S = 1$ to $S = 0$. Evidently, the energetic gain associated with the formation of the new bonds more than compensates for the cost of pairing the electrons and for the loss of Mo−Cl π-stabilization. It is expected that the strength of the new M−L bonds will affect the overall enthalpic picture. Indeed, the stronger Mo−CO bond results in a quantitative carbonylation reaction, whereas N_2 leads to an equilibrium mixture of starting material and dinitrogen adduct[18] and weaker donor molecules such as noble gases, hydrocarbons, acetone, and THF do not react. The energetics of these adduct formations have been investigated theoretically and are reported in a separate contribution, which also addresses the effect of this spin state change on the reaction kinetics.[49]

A final point of consideration is related to the different behavior of Mo and W. Baker *et al.* have reported that the reduction of Cp*WCl_4 with 3 equiv of Na in the presence of PMe_3 (a procedure identical with that in eq 1 for the synthesis of **3**) leads to the compound Cp*W(H)(Cl)$(PMe_3)(\eta^2\text{-}CH_2PMe_2)$, featuring a metallated PMe_3 ligand.[20] The formation of this product probably involves a C−H oxidative addition process on a 16-electron Cp*$WCl(PMe_3)_2$ intermediate, i.e. identical with the stable Mo product **3** (see Scheme 1). On the other hand, compound **3** fails to afford the corresponding product of PMe_3 metalation. Rather, upon warming, it decomposes, probably via a radical mechanism, to produce Cp*$MoCl_2(PMe_3)_2$ and Cp*$MoH(PMe_3)_3$ as the only identified products by NMR and EPR.

This different behavior may be attributed either to a greater kinetic barrier to the C−H oxidative addition process in the Mo case or to the greater thermodynamic

---

(40) Hooker, R. H.; Mahmoud, K. A.; Rest, A. J. *J. Chem. Soc., Dalton Trans.* **1990**, 1231−1241.

(41) Hill, R. H.; Becalska, A.; Chiem, N. *Orgtanometallics* **1991**, *10*, 2104−2109.

(42) Virrels, I. G.; George, M. W.; Johnson, F. P. A.; Turner, J. J.; Westwell, J. R. *Organometallics* **1995**, *14*, 5203−5208.

(43) Luksza, M.; Kimmer, S.; Malisch, W. *Angew. Chem., Int. Ed. Engl.* **1983**, *22*, 416−417.

(44) Gross, E.; Jörg, K.; Fiederling, K.; Göttlein, A.; Malisch, W.; Boese, R. *Angew. Chem., Int. Ed. Engl.* **1984**, *23*, 738−739.

(45) Malisch, W.; Pfister, H. *Organometallics* **1995**, *14*, 4443−4445.

(46) Morris, R. J.; Girolami, G. S. *Inorg. Chem.* **1990**, *29*, 4167−4169.

(47) Simpson, C. Q., II; Hall, M. B.; Guest, M. F. *J. Am. Chem. Soc.* **1991**, *113*, 2898−2903.

(48) Carmona, E.; Marín, J. M.; Poveda, M. L.; Atwood, J. L.; Rogers, R. D. *Polyhedron* **1983**, *2*, 185−193.

(49) Keogh, D. W.; Poli, R. *J. Am. Chem. Soc.*, submitted for publication.

Scheme 1

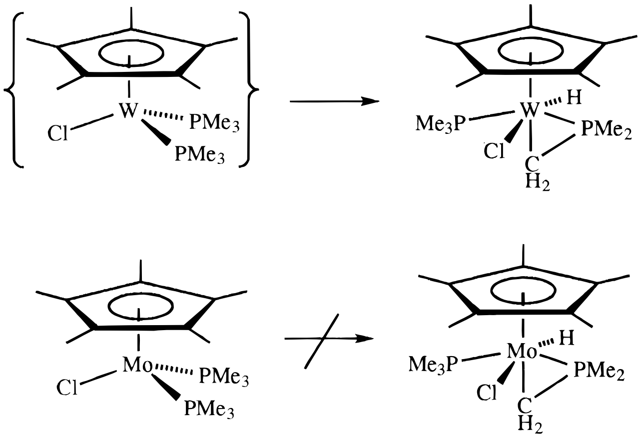

stability of the 16-electron system with respect to the product of PMe_3 metalation in the case of Mo. The effect of the spin state change on the thermodynamic picture for an oxidative-addition process should be opposite to that of a ligand addition (see Introduction), because the ideal removal of the X and Y radicals from an 18-electron $L_nM(X)(Y)$ complex leaves the metal with two unpaired electrons (triplet state). Siegbahn has explained in this manner the computational results of a lower thermodynamic gain for the oxidative addition of CH_4 to CpRh(CO) with respect to CpIr(CO), since the spin triplet starting complex is less stable by 5.9 kcal/mol for Rh and more stable by 0.3 kcal/mol for Ir.[5] Thus, while a triplet configuration for a 16-electron ML_n complex would provide thermodynamic stabilization with respect to the formation of a diamagnetic 18-electron $L_nM(L')$ adduct, it would not provide any stabilization with respect to the formation of a diamagnetic 18-electron $L_nM(X)(Y)$ oxidative-addition product. The spin state of the hypothetical 16-electron Cp*WCl(PMe_3)$_2$, let alone the magnitude of the singlet−triplet gap, is not known; therefore, the relevance of the spin state change to the different behavior of Mo and W in Scheme 1 remains undetermined. However, a more favored oxidative-addition process for the W system could also derive from an increased strength of the W−H and W−CH_2 bonds with respect to the same bonds for Mo. It is an experimental fact that oxidative-addition processes are more favored for 5d relative to 4d systems, even when there is no spin state change involved in either process (e.g. addition to square-planar Rh(I) and Ir(I) Vaska-type complexes).

Acknowledgment. We are grateful to the National Science Foundation (Grant No. CHE-9508521) for support of this work.

Supporting Information Available: For compounds **1**, **5**, and **7**, tables of crystal data and refinement parameters, fractional atomic coordinates, bond distances and angles, anisotropic thermal parameters, and H atom coordinates (27 pages). Ordering information is given on any current masthead page.

OM960331D